

RESEARCH ARTICLE

Sedimentation patterns in the Selenga River delta under changing hydroclimatic conditions

Jan Pietroń^{1,2}  | Jeffrey A. Nittrouer³ | Sergey R. Chalov⁴ | Tian Y. Dong³ | Nikolay Kasimov⁴ | Galina Shinkareva⁴ | Jerker Jarsjö^{1,2}

¹Department of Physical Geography, Stockholm University, Stockholm, Sweden

²Bolin Centre for Climate Research, Stockholm University, Stockholm, Sweden

³Department of Earth, Environmental and Planetary Sciences, Rice University, Houston, TX, USA

⁴Faculty of Geography, Lomonosov Moscow State University, Moscow, Russia

Correspondence

Jan Pietroń, Department of Physical Geography, Stockholm University, Stockholm SE-106 91, Sweden.

Email: jan.pietron@natgeo.su.se

Funding information

Marie Curie Actions, Grant/Award Number: PIRSES-GA-2012-318969; Swedish Research Council Formas, Grant/Award Number: 2012-790; National Science Foundation, Grant/Award Number: EAR-1415944; Russian Scientific Foundation, Grant/Award Number: 14-27-00083; Russian Foundation for Basic Research, project "Geochemical barriers in freshwater deltas of Russia"; Russian Foundation for Basic Research, Grant/Award Number: 15-05-05515; Bert Bolin Centre and Climate Research School

Abstract

The Selenga River delta (Russia) is a large (>600 km²) fluvially dominated fresh water system that transfers water and sediment from an undammed drainage basin into Lake Baikal, a United Nations Educational, Scientific, and Cultural Organization World Heritage Site. Through sedimentation processes, the delta and its wetlands provide important environmental services, such as storage of sediment-bound pollutants (e.g., metals), thereby reducing their input to Lake Baikal. However, in the Selenga River delta and many other deltas of the world, there is a lack of knowledge regarding impacts of potential shifts in the flow regime (e.g., due to climate change and other anthropogenic impacts) on sedimentation processes, including sediment exchanges between deltaic channels and adjacent wetlands. This study uses field measurements of water velocities and sediment characteristics in the Selenga River delta, investigating conditions of moderate discharge, which have become more frequent over the past decades (at the expense of peak flows, $Q > 1,350 \text{ m}^3 \text{ s}^{-1}$). The aims are to determine if the river system under moderate flow conditions is capable of supporting sediment export from the main distributary channels of the delta to the adjacent wetlands. The results show that most of the deposited sediment outside of the deltaic channels is characterized by a large proportion of silt and clay material (i.e., <63 μm). For example, floodplain lakes function as sinks of very fine sediment (e.g., 97% of sediment by weight < 63 μm). Additionally, bed material sediment is found to be transported outside of the channel margins during conditions of moderate and high water discharge conditions ($Q \geq 1,000 \text{ m}^3 \text{ s}^{-1}$). Submerged banks and marshlands located in the backwater zone of the delta accumulate sediment during such discharges, supporting wetland development. Thus, these regions likely sequester various metals bound to Selenga River sediment.

KEYWORDS

deltaic backwater processes, Rouse number assessments, sediment dispersal, Selenga River delta, wetland sedimentation

1 | INTRODUCTION

Delta wetlands provide important environmental services, such as sequestering sediment-bound metals through accumulation of riverine sediment, and therefore improve quality of river water discharging into the adjacent coastal zone (Day, Martin, Cardoch, & Templet, 1997; Thorslund et al., 2017). The dynamics of river water flow into a delta, as well as its sediment concentration and grain size distribution, control the magnitude and spatiotemporal variability of water storage and sediment deposition in delta wetlands (Edmonds

& Slingerland, 2010; Wright & Coleman, 1972). The sedimentation processes in the wetlands, in turn, contribute to the planform growth of a deltaic system (Rowland, Dietrich, Day, & Parker, 2009; Syvitski, Overeem, Brakenridge, & Hannon, 2012; Syvitski, Vörösmarty, Kettner, & Green, 2005). Wetlands are frequently created within the coastal area of the delta, particularly in the backwater zone where the river water stages and current flow velocity are influenced by the water level of the terminal receiving basin (Nittrouer, Mohrig, & Allison, 2011). Deltas with numerous distributary channels and complex networks are usually formed where a large sediment supply

produces channel bifurcations via avulsion processes (Syvitski & Saito, 2007); these typically possess a large number of wetland lakes that trap and store sediment.

Human activities, such as damming and land-use changes within river basins, alter water discharge patterns and sediment supply to deltas, affecting their natural storage functions (Jalowska, Rodriguez, & McKee, 2015; Nittrouer & Viparelli, 2014; Yang, Milliman, Li, & Xu, 2011). For instance, impacts of dams can lead to a recession of deltaic wetlands and subsidence of the delta plains (Syvitski et al., 2009; Yang et al., 2005). Moreover, climatic changes may influence runoff and erosion in the drainage basin, which in turn affects sediment discharge to the downstream delta (Chalov et al., 2015; Fischer, Pietroń, Bring, Thorslund, & Jarsjö, 2017; Leeder, Harris, & Kirkby, 1998; Törnqvist et al., 2014). Climate related shifts in the flow regime of rivers (e.g., magnitude of floods) can also influence the supply of sediment and its distribution within deltas (Zhao et al., 2015; Stern et al., 2016; Chalov, Thorslund, et al., 2017).

The degree of such anthropogenic and climatic forcing on a river basin is sometimes challenging to disentangle from natural variability. Furthermore, because many fluvial basins have possessed dams for many decades (see Nilsson, Reidy, Dynesius, & Revenga, 2005), natural case studies of moderate to large basins without impacts of dams are exceedingly rare. One exception is the herein studied Selenga River basin that drains into Lake Baikal (Russia). Despite the absence of dams, this system is impacted by mining activities, which locally increase soil loss from the basin that leads to significant sediment and metal contamination of the tributary streams (Jarsjö, Chalov, Pietroń, Alekseenko, & Thorslund, 2017; Pietroń, Chalov, Chalova, Alekseenko, & A., Jarsjö J., 2017; Pietroń, Jarsjö, Romanchenko, & Chalov, 2015; Thorslund et al., 2016; Thorslund, Jarsjö, Chalov, & Belozerovala, 2012). Moreover, the Selenga River basin is currently subject to climate driven shifts in hydrology and water discharge patterns. In particular, the annual maximum discharges and the annual average discharges have decreased, whereas the annual minimum discharges has increased (Chalov et al., 2015; Törnqvist et al., 2014), reducing the variability of daily discharges (see Botter, Basso, Rodriguez-Iturbe, & Rinaldo, 2013).

The Selenga River delta is a fluvially dominated fresh-water system that is characterized by up to eight orders of distributary channels; as such, the delta region has developed large lakes and widespread wetland regions that are adjacent to the channels (Lane, Anenkhonov, Liu, Autrey, & Chepinoga, 2015; Dong et al., 2016; Chalov, Thorslund, et al., 2017). The delta stores sediment (up to 40% of suspended and 70% of the total sediment load during high discharge conditions $\sim 3,000 \text{ m}^3 \text{ s}^{-1}$) and particle-bound metals originating from upstream extensive mining areas through dispersal and deposition of fine sediment where sediment-laden water evacuates distributary channels and enters adjacent low-energy wetlands (Chalov, Thorslund, et al., 2017). However, it is still unknown if and to what extent the ongoing shifts in the hydrological flow regime of the Selenga River, that is, decreased variability of daily discharges, could affect the sedimentation patterns and storage functions of the delta. Additionally, sedimentation processes of the suspended sediment load, especially with respect to grain size within the Selenga River delta and its wetlands, have yet to be investigated.

The main objective of this study is to test whether or not, under present conditions (e.g., with fewer peak flow events than before), the Selenga River is capable of supporting transport of sediment from the main channels to the adjacent wetlands within the delta, as would be typical for many deltaic systems. In addressing this objective, we also determine prevailing grain sizes of sediment and its spatial variability at storage locations within the Selenga River delta (e.g., channel banks and floodplain water bodies) at such moderate water discharge conditions.

2 | STUDY AREA

The Selenga River delta (Figure 1), located in southern Siberia, is a large ($>600 \text{ km}^2$) fluvially dominated river delta, formed on the southeast margin of Lake Baikal, which is a United Nations Educational, Scientific, and Cultural Organization World Heritage Site comprising a unique ecosystem with many endemic species. The delta is characterized by eight orders of natural distributary channels that partition water and sediment over the course of approximately 35 km. A recent study has documented that water partitioning among the channel orders produces a reduction in stream power and an associated non-linear reduction in sediment transport (Dong et al., 2016). This, in turn, produces deposition of sediment within the channel network system, with the coarsest sediment load (gravel) eventually giving way to sand and silt, starting at the delta's apex and progressing downstream to the termination of distributary channels (Dong et al., 2016; Ilyicheva, Gagarinova, & Pavlov, 2015). According to prior field observations, the main distributary channels of the delta are locally dredged, and the portions of floodplain that remains dry with exception of extreme flood events are often used for animal grazing. Additionally, the back-water zone of the delta extends upstream approximately 9 km from the delta's outlets (Dong et al., 2016), and this region is affected by intra-annual fluctuations of Lake Baikal water level (average annual amplitude of $\sim 0.7 \text{ m}$, with the lowest and highest water levels around May and September, respectively; see Figure S2), which is regulated by the operation of a dam on the Angara River near the outlet of Lake Baikal and the city of Irkutsk (Crétau et al., 2011; Chalov, Thorslund, et al., 2017; Hydroweb, 2017).

Both the Selenga River delta and basin are characterized by a continental, semidry climate with monthly mean temperatures ranging between -23.5 (January) and 16.9 °C (July; Törnqvist et al., 2014). Water flow and sediment transport regimes of the Selenga River are natural and unaffected by major engineering structures. High discharge events occur between April and October. The highest observed discharges exceed $2,000 \text{ m}^3 \text{ s}^{-1}$ and typically occur in August. During November to March, the tributaries of the Selenga River are covered with ice, and the water discharge is negligible ($80\text{--}100 \text{ m}^3 \text{ s}^{-1}$ upstream of the delta; Törnqvist et al., 2014; Chalov, Thorslund, et al., 2017). However, long term hydrological data during the period 1938 to 2009 show decreasing magnitudes of the annual maximum flows and increasing magnitudes of minimum flows at the Mostovoy gauging station, located $\sim 130 \text{ km}$ upstream of the Selenga River delta apex. Additionally, average annual water discharges significantly decreased in the Selenga River (Mostovoy station) and its headwaters

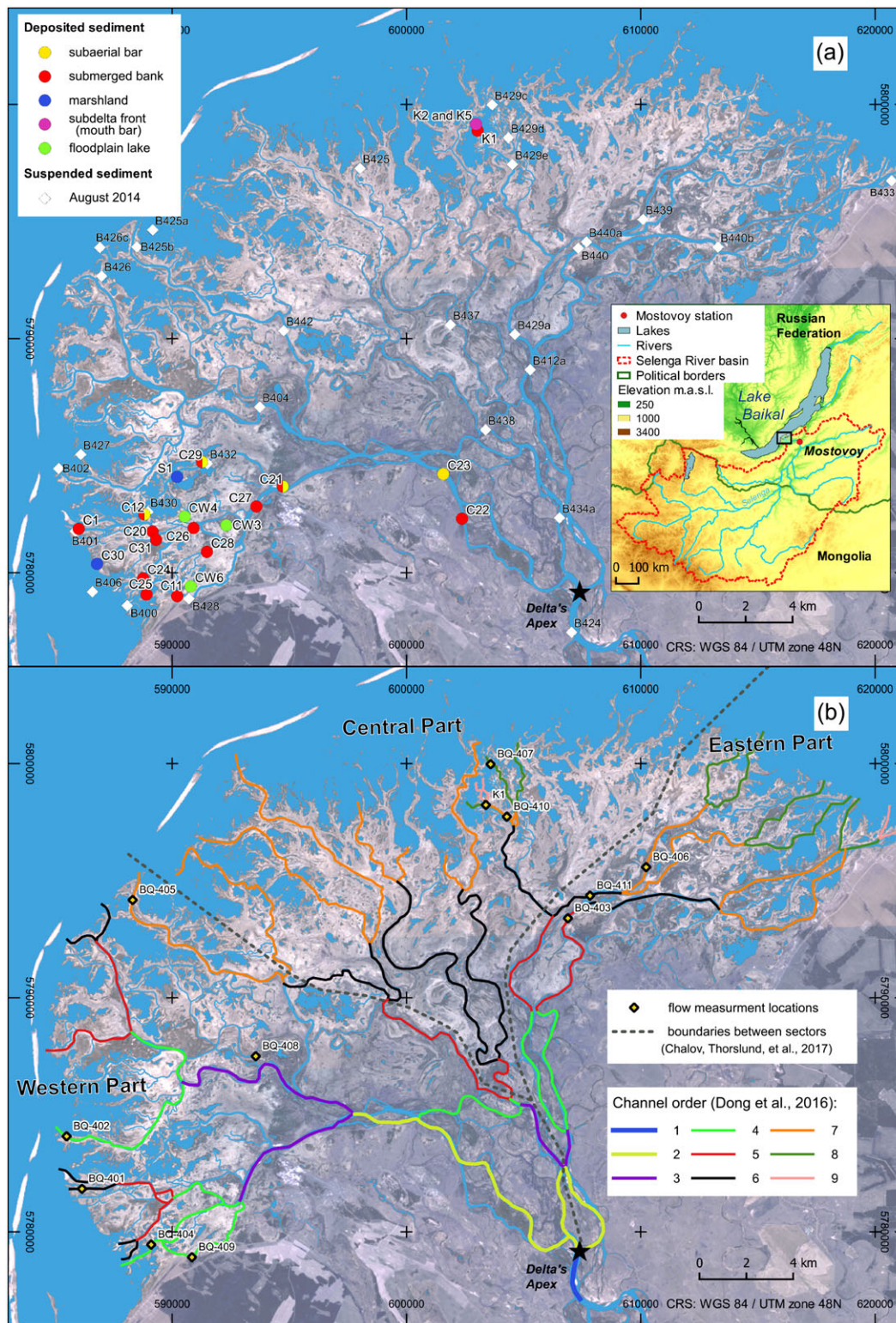


FIGURE 1 A map of the Selenga River delta: (a) locations of the sediment sampling points; (b) locations of flow measurements, classification of channel orders according to Dong et al. (2016), and division of regions in the delta according to Chalov, Thorslund, et al. (2017). Satellite image source for the background maps—LANDSAT (bands 2, 3, and 4) from 30th of May 2014 (U.S. Geological Survey, 2015); the blue background indicates wetted areas (see Section S1). Inset map in part (a): location of the Selenga River delta in the Selenga River basin (red border); elevation model—Shuttle Radar Topography Mission 90 m (U.S. Geological Survey, 2012)

(Ulaanbaatar, Mongolia) after mid-1990 (Chalov et al., 2015; Pietroń et al., 2015). These conditions are associated with a changing basin hydroclimate and also coincide with thawing permafrost and an increase in the average annual temperature by 1.6 °C (Törnqvist et al.,

2014). Land use in the Selenga River basin has also changed (e.g., loss in cultivated area in the Russian part of the basin since the 1980s; Bazhenova & Kobylkin, 2013). A notable net effect of such ambient changes is the significant decrease in the annual sediment discharge

to the Selenga River delta, as measured over the last 30 years (Chalov et al., 2015; Potemkina, 2011).

The Selenga River delta functions as an important filter of water flowing from the Selenga River basin into Lake Baikal. In particular, the wetland-dominated areas of the delta between the distributary

channels retain sediment and associated metal pollutants (Chalov, Thorslund, et al., 2017). These areas are characterized by numerous water bodies that are classified in terms of hydrological connectivity to distributary channels. Floodplain water bodies with no direct overland connection to a distributary channel during moderate flow



FIGURE 2 Examples of different water bodies and wetlands within the Selenga River delta (pictures by Jerker Jarsjö, Jan Pietroń, and Tian Dong). GoogleMaps images were extracted using R package “RgoogleMaps” (Loecher, 2014). Left bottom corners—approximate location (WGS 84 / UTM 48 N) of the areas

conditions (discharges around the mean values) are denoted as closed lakes (Figure 2). Floodplain lakes connected to a distributary channel via a tie channel provide a pathway for water and sediment to exchange; such lakes are therefore defined as “active.” Open water bodies that are adjacent to delta channels so as to convey water during average flow conditions are defined as marshlands. These water bodies are typically located at the delta fringe (i.e., within the backwater zone) and are subject to changing conditions of water and sediment discharge from distributary channels, depending on water discharge from the Selenga River. Over time, water bodies may change function. For example, lakes on the Selenga River delta can be converted to floodplain lakes or marshlands by connection to an avulsed channel (e.g., Kazanova branch, Figure 1; Ilyicheva et al., 2015). In such circumstances, nourishment of marshlands with sediment can lead to a formation of net sedimentation areas characterized by small versions of natural delta lobes (denoted subdeltas, Figure 2d; see Mjos, Walderhaug, & Prestholm, 1993; Dean, Wells, Fernando, & Goodwin, 2013). In time, the newly deposited material can be colonized by marshland vegetation (Cahoon, White, & Lynch, 2011).

3 | MATERIAL AND METHODS

3.1 | Data acquisition, processing, and analysis

Daily water discharge data (Q , $\text{m}^3 \text{s}^{-1}$) of the Selenga River were obtained from the Hydro-meteorological Centre of Russia at the Mostovoy gauging station (see Chalov et al., 2015; Törnqvist et al., 2014). These long-term data were divided into two different periods, representing the hydrological flow regime of the Selenga River before (1975–1994) and after (1995–2014) the on-set of current draught conditions (Chalov et al., 2015) and used in analyses of differences in daily discharge patterns between the periods. Measurements of water discharge for the delta's distributary channels were collected between the 6th and 18th of August 2014, and on the 9th of August 2016 (Figure 1b). Water stream velocity and discharge measurements in 2014 were collected using propeller-type velocity current meters deployed from boats. Associated discharge conditions were estimated using a trapezoidal rule described by Jarsjö et al. (2017). The water surface velocity measurements in 2016 were collected using the float method, whereby data were corrected (a factor $\phi = 0.91$) for sand-bed channels to estimate depth-average velocities (Gutry-Korycka & Werner-Więckowska, 1996).

Suspended sediment concentrations were measured between 28th of July and 18th of August 2014, at midstream locations of the delta's distributary channels (33 samples across the entire delta; locations shown in Figure 1a). Depth-integrated water samples (at the surface water layers) were collected with 2-L plastic sampling bottles. The water was filtered using preweighed membrane filters (with pore size $0.45 \mu\text{m}$) and vacuum pumps (Millipore). Afterwards, filters and associated sediment were oven dried. Grain size analyses of the suspended sediment samples were conducted using a laser granulometer (Fritsch Analysette 22; reflecting volumetric distributions) at Moscow State University (Russia). Prior to the grain size analysis, all samples were treated with sodium pyrophosphate

($\text{Na}_4\text{P}_2\text{O}_7$) to disintegrate flocs (see Bates, Coxon, & Gibbard, 1978). The obtained data were classified according to a Russian grain size system (see Shein, 2009; Figure S3).

Sediment samples were collected during a field campaign at the western part of the Selenga River delta (Figure 1) between August 21st and 23rd, 2014. Twenty-one sediment samples were taken within the western part of the delta (locations shown in Figure 1a). This part conveys a considerable portion (~30%) of the total water discharge of the Selenga River during high flow conditions ($Q \sim 2,700 \text{ m}^3 \text{ s}^{-1}$) and even more (up to ~50%) during the lower flows of summer ($Q \sim 1,200 \text{ m}^3 \text{ s}^{-1}$). In general, this part of the delta, in conjunction with the eastern part, conveys most of Selenga River's water and sediment discharge (75–89% of the water discharge; Chalov, Thorslund, et al., 2017). The western delta part comprises a variability of wetland types (i.e., shrub areas, sedge-cane meadows as well as cane/aquatic vegetation bogs and waterlogged territories), which is representative for the entire delta area (Ilyicheva et al., 2015).

The sampling locations (Figure 1a) consisted of (a) submerged banks (C1, C11, C12, C12, C20, C20, C22, C24, C25, C26, C27, C28, C29, and C31), (b) subaerial sand bars located in the primary distributary channels (C12b, C21b, C23b, and C29b), (c) bed sediment samples from marshlands (C31 and S1), and (d) the floodplain lakes (active: CW4 and CW6 and closed: CW3; see Section 2). Three samples from submerged banks (C12*, C20*, and C21*) were taken on 4th of September 2013. The term “submerged banks” refers to marginal areas of confined channels or areas of subaqueous levees formed in unconfined channels. These locations were chosen to measure the characteristics of sediment deposits at the interface (border) between the main channels and adjacent wetlands. The locations are likely to remain inundated despite transient flow and Lake Baikal water level conditions. Most of the submerged bank locations (except C21, C22, and C27) were sampled within the backwater zone of the delta (up to ~9 km from the delta's outlets; Dong et al., 2016). All locations were inundated during the time of sampling. The area of the backwater zone, however, may vary depending on the changes in water level of Lake Baikal (Figure S2), which was approximately 6.0 cm below the August average level (455.61 m a.s.l. for period 1993–2013) around the time of sediment sampling in 2014 (16th of August 2014; Hydroweb, 2017). In addition, the sampled sediment locations at the delta front can be subject to wind waves, as observed by Chalov, Bazilova, and Tarasov (2017).

All of the sediment sampling sites were accessed via boat or by foot. Floodplain lakes were sampled approximately 2 m from their shore. A sampler capable of collecting the upper 5–10 cm of the surface sediment was used in submerged and inaccessible locations. Samples from accessible but submerged areas and subaerial bar sediment were collected using a spatula to recover the upper 5–10 cm. Each sample was well-mixed and then oven dried ($60 \text{ }^\circ\text{C}$) in a scientific field station located close to the delta (in the village of Istomino), before being transported to Stockholm University (Sweden). The well-mixed samples were dried in $150 \text{ }^\circ\text{C}$ for 24 hr. Around 5.0 g of each sample was separated to analyse the organic matter content (OM, %), utilizing loss upon ignition method (6 hr in $550 \text{ }^\circ\text{C}$), where (based on Delteus & Kristiansson, 1995)

$$OM (\%) = \frac{\text{pre_ignition weight (g)} - \text{pos_ignition weight (g)}}{\text{pre_ignition weight (g)}} 100 (\%). \quad (1)$$

Afterwards, the grain size composition of the remaining sample was measured using hydrometer analysis (measurement of the weight distribution; Delteus & Kristiansson, 1995). The material coarser than 74 μm was partitioned for grain-size analysis using a set of stainless steel sieves. Prior to this analysis, all samples were treated with sodium pyrophosphate ($\text{Na}_4\text{P}_2\text{O}_7$) to disintegrate flocs that could arise due to OM (Bates et al., 1978; Delteus & Kristiansson, 1995). Additionally, samples recognized to contain more than ~5.0% of OM were subject to a 30% solution of hydrogen peroxide (H_2O_2) to reduce the OM content (Simon Fraser University, 2012). To test the possible effects of OM in the samples that were not treated with H_2O_2 , the (uncorrected) results of the analysis were compared with corrected results using an equation proposed by Gasparotto et al. (2003; Section S2). The estimates show that, on average, the clay content could have been underestimated by a relatively modest 0.4 percentage points from 16.3% (0.8 percentage point from 14.8% for submerged banks).

Additionally, three sediment deposits were sampled on the 9th of August 2016, from the mouth bar deposit of the Kazanova branch (locations shown in Figure 1a), which represents an active avulsion into the central sector of the Selenga River delta. The measurements were carried out at a submerged bank (K1) and an inundated front of the subdelta (mouth bar, K2, and K5). Grain size distribution of each sample was measured using a Malvern Mastersizer 2000 (for material <63 μm) and Retsch Technology CAMSIZER (for material >63 μm) at Rice University (TX, USA; measurement of the volume distribution). Prior to the grain size analysis, all samples were treated by sodium pyrophosphate ($\text{Na}_4\text{P}_2\text{O}_7$) to disintegrate flocs (see Bates et al., 1978). Around 10 g of each sample was oven-dried (> 12 hr in 90 $^\circ\text{C}$) and used to measure the OM utilizing loss upon ignition method (> 8 hr in 400 $^\circ\text{C}$) as described above (Equation 1).

Linear interpolation between measurement data points on cumulative grain size distribution curves (Figure S3) was used to estimate fractional contributions of clay (<3.9 μm), silt (3.9–63 μm), and sand (63–2,000 μm) for given particle sizes, as well as statistical quantities, such as median grain size (D_{50}), of the sampled sediment (Seward-Thompson & Hails, 1973; Shein, 2009). This method was also used to report all considered sediment data in a common grain size classification according to Wentworth (1922; Table S1).

To quantify the degree of grain size variability in the deposited and suspended sediment samples, the Inclusive Graphic Standard Deviation (σ_ϕ) is used as a measure of sorting (Folk & Ward, 1957)

$$\sigma_\phi = \frac{\phi_{84} - \phi_{16}}{4} + \frac{\phi_{95} - \phi_5}{6.6}, \quad (2)$$

where ϕ_n is the n percentile of the grain size distribution in the Krumbein phi (ϕ) units. The ϕ of a grain size D (mm) is defined as $\phi = -\log_2 D/D_0$, where D_0 is a reference diameter 1.0 mm. The degree of sorting is defined by the following σ_ϕ ranges: $\sigma_\phi < 0.35$, *very well sorted*; $\sigma_\phi = 0.35 - 0.50$, *well sorted*; $\sigma_\phi = 0.50 - 1.0$, *moderately sorted*; $\sigma_\phi = 1.0 - 2.0$, *poorly sorted*; $\sigma_\phi = 2.0 - 4.0$, *very poorly sorted*; and $\sigma_\phi > 4.0$, *extremely poorly sorted* (Krumbein & Aberdeen, 1937).

Additionally, the Mann-Whitney U -test was used in the study to determine the differences in statistical significance between the median values representing different categories of the studied datasets (e.g., deposited sediment samples). The categories represented by too few samples ($n < 6$; Townend, 2013) were grouped with a similar category, if available or omitted from the statistical analysis.

3.2 | Rouse number analysis

A dimensionless Rouse number (Pn) is used to determine the threshold of suspension for bed-material sediment (e.g., sand, >63 μm ; Colby, 1957) during flood (bankfull) and moderate flow conditions (e.g., Middleton & Southard, 1984; see Section 3.1 regarding Q measurements):

$$Pn = \frac{\omega_s}{\kappa u_*}, \quad (3)$$

where, ω_s is settling velocity (m s^{-1}) of the sediment, which is a function of grain size, shape, and density (Dietrich, 1982; see Section S3), κ is von Karman's constant (0.41), and u_* is shear velocity (m s^{-1}). Values lower than the critical Rouse number $Pn^* = 2.5$ indicate that a sediment particle begins to contribute to the suspended load (Middleton & Southard, 1978; Huston, 2014), whereas higher values indicate that a sediment particle is most likely transported as part of the bed load (Lynds, Mohrig, Hajek, & Heller, 2014). Herein, shear velocity is estimated as $u_* = \sqrt{\tau_b/\rho}$, where ρ is the fluid density (kg m^{-3}), and τ_b is the boundary shear stress (Pa). Minimum, median, and maximum boundary shear stress values during bankfull flow conditions for the Selenga River delta channels are based on values reported by Dong et al. (2016; see Table S2).

The u_* values are also independently computed from depth-average flow velocity values U (m s^{-1}) measured within the Selenga River delta during the 2014 and 2016 field campaigns (during which moderate flow conditions prevailed; Section 3.1):

$$u_* = U\sqrt{C_f}, \quad (4)$$

where C_f is a dimensionless friction coefficient (Nittrouer et al., 2012) estimated using the Manning-Strickler formula (Parker, 1991): $C_f^{-1/2} = \alpha_r(H/(n_k D_{90}))^{1/6}$, where α_r is a dimensionless constant equal to 8.1, H is the average measured channel depth (m), n_k is a dimensionless constant equal to 2.0, and D_{90} is the sediment size (nominal grain diameter) coarser than 90% of the bed material grain size distribution. Values of D_{90} are based on bed sediment sample sizes for different channel orders classified in Dong et al. (2016) using patterns of channel bifurcations (Hack, 1957). The average channel depth is estimated as $H = A/W$, where A and W are the channel flow area (m^2) and width (m) measured during the discharge measurements, respectively (Section 3.1).

Settling velocities (ω_s) used in Equation 3 are evaluated for sediment sizes coarser than 10%, 50%, and 90% of the cumulative sediment grain size distribution of the bed material at submerged bank locations (D_{B10} , D_{B50} , and D_{B90} , respectively). The D_{B10} , D_{B50} , and D_{B90} are estimated using linear interpolation between the measured or reported values from the cumulative grain size distribution for each considered sediment sample (see Section 3.1). Channel order

for each of the submerged bank samples are identified, as well as the minimum, average, and maximum D_{B10} , D_{B50} , and D_{B90} for each channel order.

4 | RESULTS

4.1 | Observed hydrological conditions

Depth-averaged channel velocities and the corresponding water discharges during the time of suspended load sampling (August 2014) range between $U = 0.14\text{--}0.69\text{ m s}^{-1}$ and $Q = 4.3\text{--}124\text{ m}^3\text{ s}^{-1}$, respectively (Table 1). Additional measurements from August 2016 resulted in $U = 0.14\text{ m s}^{-1}$ and $Q = 4.3\text{ m}^3\text{ s}^{-1}$ at one of the outlets (14 m wide) of the subdelta located in a seventh-order channel (K1). The measured current velocities within the open water body of the subdelta front are $U = 0.05\text{--}0.31\text{ m s}^{-1}$.

Daily water discharge values and frequencies at the Mostovoy gauging station near the Selenga River delta (Figure 1b) indicate major changes in the Selenga River's hydrological flow regime between the periods 1975–1994 and 1995–2014 (Figure 3). For instance, the average daily discharge decreased from $893\text{ m}^3\text{ s}^{-1}$ in the former period to $725\text{ m}^3\text{ s}^{-1}$ during the recent 20 years. Also, the standard deviation of the daily water discharges decreases from $\sigma = 937\text{ m}^3\text{ s}^{-1}$ for 1975–1994 to $\sigma = 665\text{ m}^3\text{ s}^{-1}$ for 1995–2014. Moreover, water discharge data from the two periods (1975–1994 and 1995–2014) indicate that the average daily discharges of $50\text{--}300\text{ m}^3\text{ s}^{-1}$ occur during 41% of the period (i.e., 149 days/year, Figure 5). The relative frequency of intermediate discharges ($450\text{--}1,350\text{ m}^3\text{ s}^{-1}$) increased from 26% (1975–1994) to 40% (1995–2014). The largest increase within this intermediate range of flows is for discharges between 750 and $1,250\text{ m}^3\text{ s}^{-1}$ (moderate flows; 17% to 27%). However, the frequency of high discharges (i.e., $>1,350\text{ m}^3\text{ s}^{-1}$) decreased from 26% to 16%. Additionally, the greatest relative decrease is within this range of daily discharges greater than $2,800\text{ m}^3\text{ s}^{-1}$ (from 5.6% to 0.99%). The maximum discharges for the periods of 1975–1994 and 1995–2014 were 7,090 and $6,420\text{ m}^3\text{ s}^{-1}$, respectively.

The mean daily discharge at Mostovoy gauging station during the period of sediment sampling in 2014 (from 28th of July to 23rd of August) varied between $984\text{--}1,191$ and $914\text{--}946\text{ m}^3\text{ s}^{-1}$, respectively (Figure 4). The mean daily discharge during the sampling in 2013 (on 4th of September) is $2,700\text{ m}^3\text{ s}^{-1}$. These sampling periods were included in the discharge frequency analysis (period 1995–2014; Figure 3). The mean daily discharge during the August 2014 campaign fell into the interval 900 to $1,200\text{ m}^3\text{ s}^{-1}$. During the past 20 years (1995–2014), these discharges occurred 19% of the period (69 days/year), about 7.2% more than of the former 20 years (1975–1994; Figure 3). The discharges during the 2013 campaign (between $2,650$ and $2,750\text{ m}^3\text{ s}^{-1}$) occur only for about 0.37% during the past 20 years (around 1 day/year), about 0.36% less than during the former 20 years (1975–1994; Figure 3).

4.2 | Properties of the deposited and suspended sediment

The median grain size (D_{50}) range, the average (\bar{x}) grain size D_{50} , and the number (N) of sediment deposit samples vary among categories of sample locations within the Selenga River delta as follows: submerged banks ($D_{50} = 12\text{--}77\text{ }\mu\text{m}$, $\bar{x} = 37\text{ }\mu\text{m}$, $N = 16$), subaerial sand bars ($D_{50} = 72\text{--}210\text{ }\mu\text{m}$, $\bar{x} = 140\text{ }\mu\text{m}$, $N = 4$), floodplain lakes ($D_{50} = 4.3\text{--}6.8\text{ }\mu\text{m}$, $\bar{x} = 5.2\text{ }\mu\text{m}$, $N = 3$), marshlands ($D_{50} = 19\text{--}26\text{ }\mu\text{m}$, $\bar{x} = 23\text{ }\mu\text{m}$, $N = 2$), and the delta mouth bar ($D_{50} = 84\text{--}113\text{ }\mu\text{m}$, $\bar{x} = 98\text{ }\mu\text{m}$, $N = 2$). The U -test showed that the median D_{50} of subaerial sand bar samples and mouth bar samples is significantly lower ($p \leq .05$) than the median of submerged bank samples and marshland samples, which implies different sedimentation characteristics between the groups. The D_{50} of the sand bar samples decreases with increasing distance from the delta's apex (e.g., $208\text{ }\mu\text{m}$ at C21b to $70\text{ }\mu\text{m}$ at C12b), which is consistent with the finding of sediment fining patterns of bed material in the Selenga River delta (Dong et al., 2016). The approximate distances from the nearest main channel to the marshland and floodplain lake sampling locations are 170 m for S1, 220 m for C31, 370 m for CW3, 430 m for CW4, and 320 m for C31.

TABLE 1 Summary of flow measurements (velocity U , m s^{-1} and discharge Q , $\text{m}^3\text{ s}^{-1}$) at different locations in the Selenga River delta during field campaigns in 2014 and 2016

Measurement point (associated sediment deposit sampling location)	Channel order ^a	Date of a measurement (day-month-year)	Channel width, W (m)	Average flow depth H (m)	Average velocity, U (m s^{-1})	Discharge, Q ($\text{m}^3\text{ s}^{-1}$)
BQ-407	8	16-08-2014	50	2.1	0.19	20.8
BQ-405	7	13-08-2014	65	0.9	0.21	12.9
BQ-410		16-08-2014	65	1.3	0.48	40.9
K1 (K1)		09-08-2016	14	0.6	0.19	1.5
BQ-406	6	15-08-2014	40	0.4	0.32	5.2
BQ-411		15-08-2014	110	1.6	0.69	125
BQ-401 (C1)	5	06-08-2014	50	1.9	0.36	33.6
BQ-403		09-08-2014	120	0.9	0.46	50.2
BQ-402	4	06-08-2014	20	1.5	0.14	4.3
BQ-404 (C25)		12-08-2014	45	2.3	0.24	24.6
BQ-409 (C11)		18-08-2014	45	1.8	0.43	35.4
BQ-408	3	18-08-2014	85	2.1	0.65	116

Note.

^aChannel orders according to Dong et al. (2016)

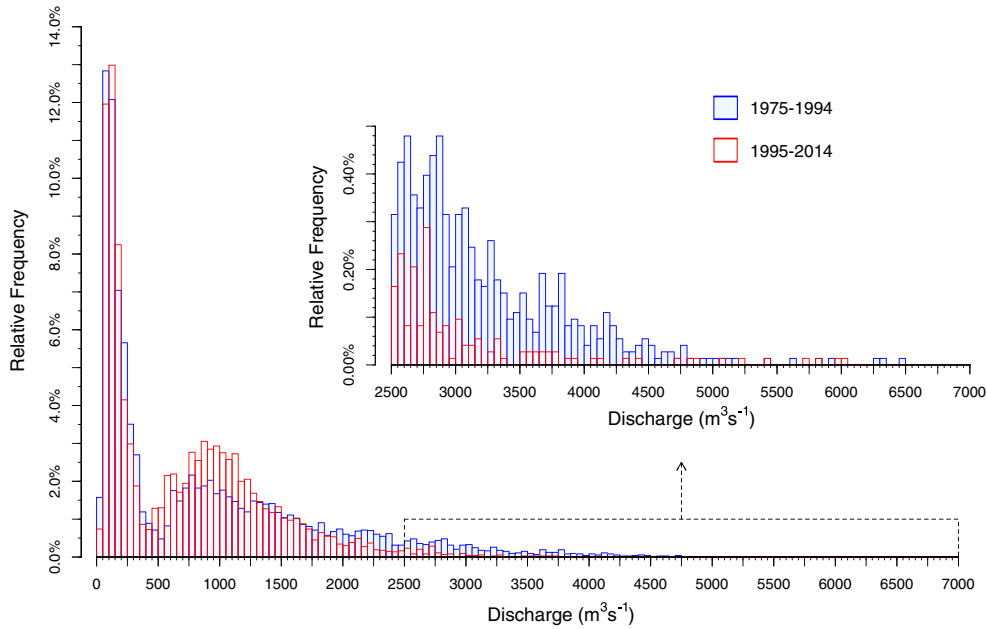


FIGURE 3 Comparison between frequencies of daily water discharges for the periods of 1975-1994 (blue bars) and 1995-2014 (red bars)

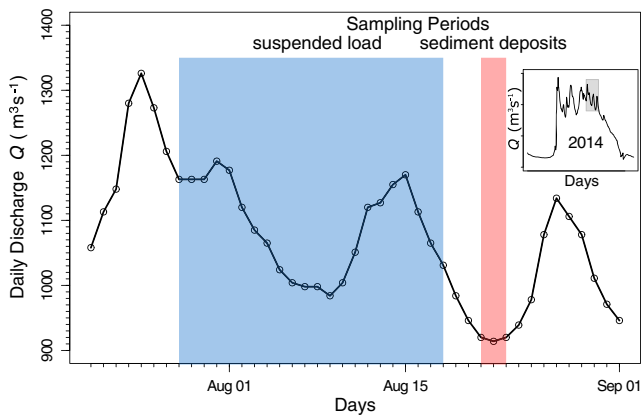


FIGURE 4 Discharge conditions upstream of the Selenga River delta (Mostovoy station) during sampling periods indicated by the background colours: blue – period of suspended load sampling, red area – sediment deposits sampling

On average, the submerged bank samples contain 15% clay, 57% silt, and 28% sand (red points in Figure 5). However, it is noted that three of the samples (C11, C20, and C28) contain a high proportion of clay (about 29%). The submerged bank samples are characterized by a large range of sand content, from 8.9% to 55%. The sand fraction for submerged bank samples varies from very fine sand to very coarse sand. The submerged bank sample from location C22 is characterized by the deposition of very fine pebble gravel (2,000–4,000 μm ; not shown in Figure 3). The submerged bank samples are poorly to very poorly sorted ($\sigma_\phi = 1.5\text{--}2.3$, average = 1.9). The sand bar samples (black crosses, Figure 5) contain 3.5% clay and 14% silt. Sand constitutes between 59% (C12b) and 94% (C29b) of the samples, and they are moderately to poorly sorted ($\sigma_\phi = 0.6\text{--}1.6$, $\sigma_\phi = 1.1$).

Floodplain lakes possess very fine sediment; on average, 45% to 52% of the samples are comprised of clay and silt (green squares in Figure 5). The marshlands contain 24% clay and 64% of silts (blue

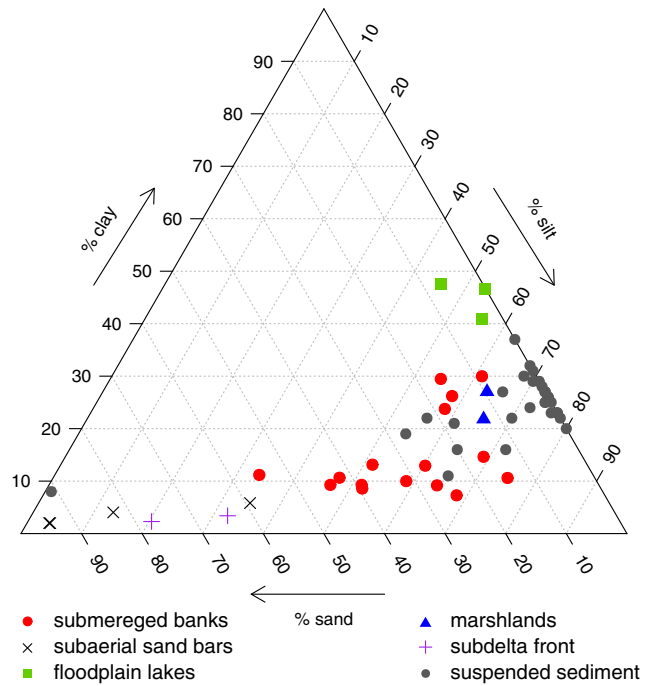


FIGURE 5 Size distribution of the deposited and suspended sediment of the Selenga River delta—division between % of clay (<3.9 μm), % of silt (3.9–63 μm), and % of sand (63–2000 μm); More detailed grain size distribution of the samples is located in Table S4 and S5, and Figure S3

triangles in Figure 5). On average, 3.5% and 11% of the samples from the floodplain lakes and marshlands, respectively, are sand (Figure 5). Interestingly, although in both sampled marshlands, the coarsest fraction is fine sand (125–250 μm), in the case of floodplain lakes, the coarsest sand varies from very fine sand (63–125 μm) in the closed floodplain lake (CW3) to fine and medium sand (up to 500 μm) in the active lakes (CW4 and CW6). An explanation for this observation may be that channelized flow connecting distributary channels to

active lakes maintains a greater sediment transport capacity than unconfined flows nourishing closed lakes. On average, the samples from floodplain lakes and marshlands are poorly ($\sigma_\phi = 1.8$) and very poorly sorted ($\sigma_\phi = 2.2$), respectively. The sampled delta mouth bar (subdelta front; Figure 1a) is on average 2.9% clay and 26% silt (locations K2 and K5; purple crosses in Figure 5). Samples from these locations possess mainly sand (71% of the sample, the coarsest sediment found at these locations is medium sand), and they are poorly sorted ($\sigma_\phi = 1.5$).

The average measured OM of the deposited sediment at different sampled locations is 4.5% (submerged banks), 0.76% (subaerial sand bars), 16% (closed and active floodplain lakes), 6.5% (marshlands), and 3.1% (subdelta front). OM is well correlated with the percentage of clay ($<3.9 \mu\text{m}$; $R^2 = 0.80$, linear regression; Figure 6). From visual inspection of Figure 6, it can be seen that the floodplain lakes have much higher OM, which is likely due to a local production of organic matter in these lakes (see Meyers & Ishiwatari, 1993). Excluding floodplain lake samples from the dataset yields a stronger correlation with the percentage of clay ($R^2 = 0.89$, logarithmic regression, see Figure S1). In addition, the U -test showed that the median OM of the subdelta front and subaerial sand bar samples is significantly different ($p \leq .05$) from the average of submerged bank and marshland samples.

The D_{50} of measured suspended sediment is $32 \mu\text{m}$. The D_{50} of the suspended load measured upstream of the delta apex on August 3rd is $7.2 \mu\text{m}$. On average, suspended sediment (grey points, Figure 5) consisted of 24% clay ($<3.9 \mu\text{m}$) and 68% silt ($3.9\text{--}63 \mu\text{m}$). The suspended sediment, on average, contained about 7.3% sand ($>63 \mu\text{m}$). However, 21 of 32 samples contain less than 1.0% sand, and six samples contain no sand. More detailed grain size distribution of all samples is in Tables S3 and S4. The suspended sediment is poorly to extremely poorly sorted ($\sigma_\phi = 1.6\text{--}3.8$, average = 2.1).

The sediment sizes coarser than D_{B10} , D_{B50} , and D_{B90} of bed material for submerged bank samples are presented in Table 2. The average values of D_{B10} and D_{B50} for all samples are 70.2 and 101 μm , respectively. The corresponding average D_{B90} is 148 μm . The results of the U -test showed that there are no significant differences ($p > .05$) between the medians of the D_{B10} , D_{B50} , and D_{B90} values between the groups of channel Orders 2–4 and 5–7. This result implies similar gradation of sand in submerged banks across the delta area. As shown

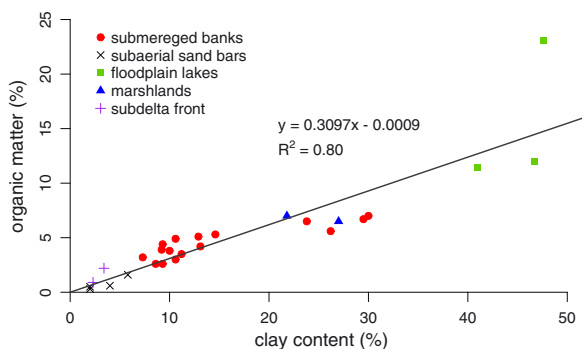


FIGURE 6 Measured percentage (%) of clay ($<3.9 \mu\text{m}$) versus organic matter content (OM) of all sediment samples

TABLE 2 The D_{10} , D_{50} , and D_{90} (μm) of the sand-gravel material (D_{B10} , D_{B50} , and D_{B90}) of submerged bank samples

Location	Channel order ^a	Grain size distribution of sediment $>63 \mu\text{m}$		
		D_{10} (μm)	D_{50} (μm)	D_{90} (μm)
K1	7	69.1	95.7	122
C1	5	69.1	95.4	122
C20		69.1	95.5	122
C20*		69.0	94.8	121
C24		68.9	94.7	121
C31		72.6	113	220
C11	4	68.9	94.6	120
C12		68.9	94.7	120
C12*		70.2	101	185
C25		69.8	98.9	163
C26		69.4	96.8	124
C28		69.4	96.8	124
C29		74.5	123	225
C21*	3	71.3	107	212
C27		68.9	94.7	120
C22	2	73.7	118	2,897

Note.

^aChannel orders according to Dong et al. (2016)

by the D_{B10} , D_{B50} , and D_{B90} values, almost all samples are dominated by very fine sand. The coarsest fractions are usually fine or medium sand (see Table S3). Hence, the bed material represented by the submerged bank samples is very well to moderately sorted ($\sigma_\phi = 0.17\text{--}0.60$, average = 0.38).

4.3 | Shear velocities and potential for suspended sediment transport

4.3.1 | Bankfull flow conditions

There are five orders of distributary channels in the studied western sector of the Selenga River delta (Dong et al., 2016). Five submerged bank samples were taken in fifth-order channels, seven in fourth, two in third, and one in a second-order channel. A channel in the subdelta (near location K1, Section 2 and Figure 1) is classified as a seventh-order channel. The shear velocity values (u_*) for bankfull flow conditions are alike for all third–fifth-order channels (Figure 7a) and range $0.02\text{--}0.08 \text{ m s}^{-1}$. The values for the second-order channel are $0.07\text{--}0.09 \text{ m s}^{-1}$, and the values for the seventh-order channel are $0.01\text{--}0.03 \text{ m s}^{-1}$. The corresponding estimated Rouse numbers (P_n) for the average D_{B10} , D_{B50} , and D_{B90} are lower than the critical value $P_n^* = 2.5$ in third–fifth- and seventh-order channels. Only the P_n values for the maximum D_{B90} and the lowest u_* values exceed the critical value. Hence, the results imply that for bankfull flow conditions, up to 90% of the coarse sediment ($>63 \mu\text{m}$) from the submerged banks in the third–seventh-order channels could be conveyed to these locations as part of suspended-load transport. The P_n values for the second-order channel suggest that sediment grain size characteristics for the D_{B10} and D_{B50} can be transported in suspension, but the coarsest particles characteristic for D_{B90} are likely to remain as bedload.

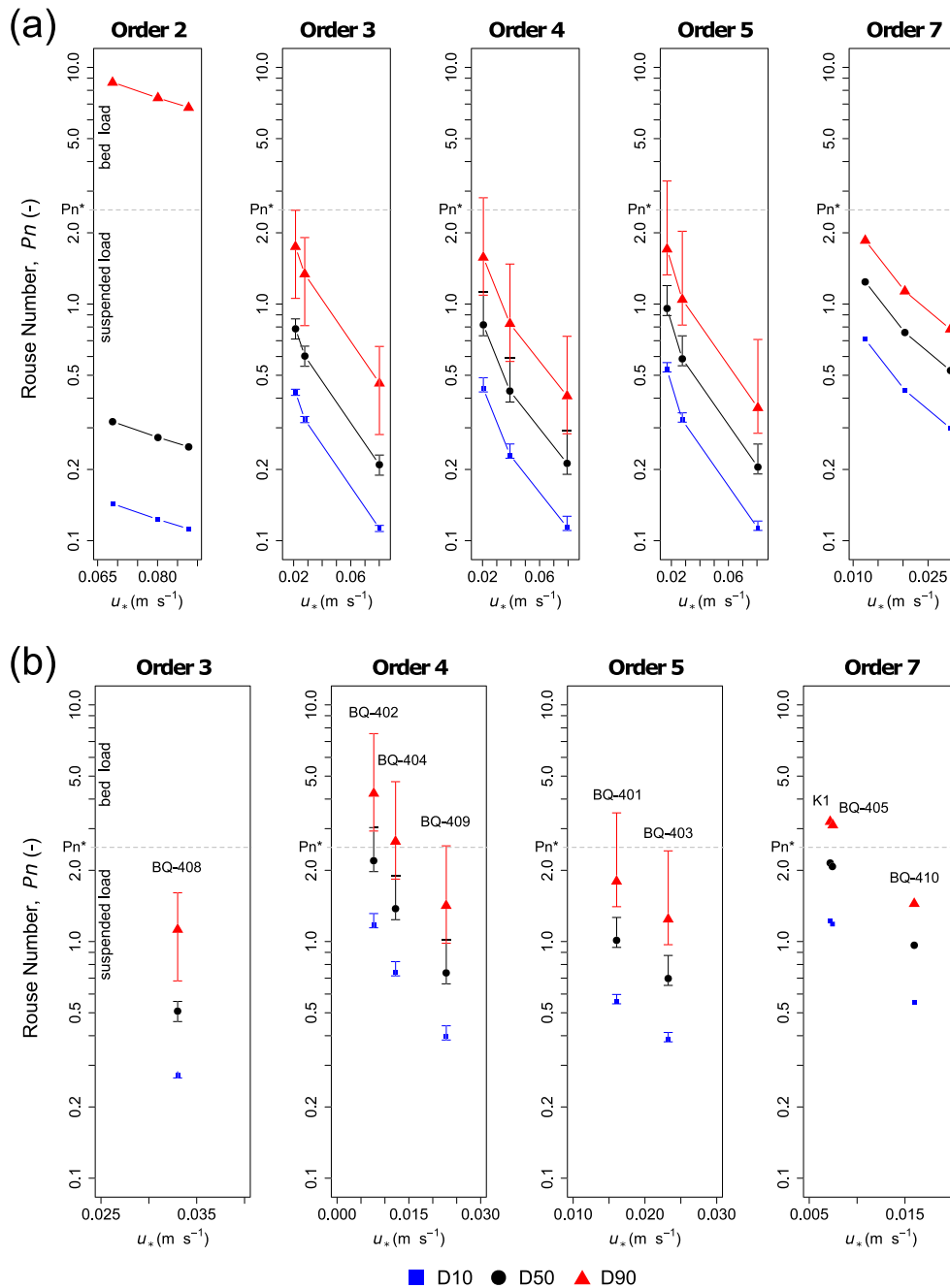


FIGURE 7 Rouse numbers (P_n) for different channel orders in the Selenga River delta for shear velocity values u_* (m s⁻¹) representing: (a) bankfull flow conditions and (b) in situ measurements of depth-average flow velocities. The presented P_n values are for the average and extreme (whiskers) D_{10} , D_{50} , and D_{90} of the sand-gravel material (DB_{10} , DB_{50} , and DB_{90}) of submerged bank samples within different channel orders

4.3.2 | Moderate flow conditions of the field measurement period

Values of u_* corresponding to flow conditions during the time period of measurements presented herein (Section 4.2) are generally within the lower range of the u_* values for bankfull flow conditions (Figure 8). Only two measurement-based shear velocity values are above the median u_* values under bankfull flow conditions. The Rouse number (P_n) results are focused in the third–fifth and seventh channel orders, for which the measurement-based u_* values and the DB_{10} , DB_{50} , and DB_{90} are available (Figure 7b). The estimated P_n values for the average DB_{10}

and DB_{50} are lower than the critical value (i.e., $P_n^* = 2.5$) for all sampling locations under the water discharge of sampling period. Only the P_n values for the maximum DB_{50} at location BQ-402 (fourth-order channel) are greater than the P_n^* . The P_n values for the average DB_{90} are lower or greater than the P_n^* depending on location. Generally, for the flow conditions during field measurements, more than 50% of the sand sediment (>63 μ m) from the submerged banks in third–seventh-order channels was likely conveyed to the sampling locations in suspension. The part of the submerged bank sediment that could not be transported in suspension during such flow conditions (Figure 7b) was likely transported as bed load or in suspension during bankfull discharge

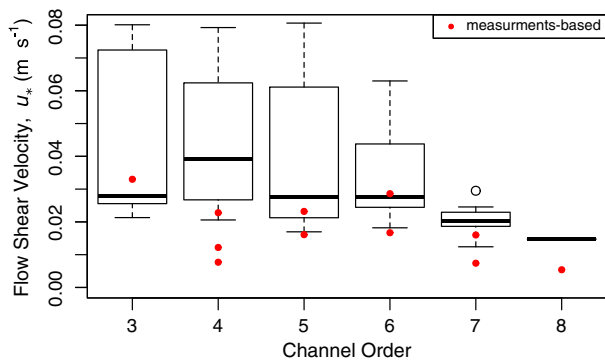


FIGURE 8 Shear velocity values (u_* , m s^{-1}) for different channel orders: the red points are computed u_* -values based on measurements of depth-average flow velocity collected during the 2014 field campaign; the box plots are based on data reported by Dong et al. (2016). According to the U -test, there are no significant difference ($p > .05$) between medians of data representing the box plots for Orders 3–6, however, there are significant differences ($p \leq .05$) between medians of data for Order 7 in contrast to the channel Orders 3–6

conditions (characterized by higher u_* ; Figure 7a). All estimated Pn values are shown in Tables S5 and S6.

5 | DISCUSSION

The data presented herein show that the submerged bank areas are characterized by a large proportion of clay and silt (70%, sample weight). These areas are also characterized by a considerable proportion of well-sorted bed-material sediment (i.e., sand) with a dominant fraction of very fine sand (63–125 μm), as inferred from the average $D_{B10} = 70.2 \mu\text{m}$ and $D_{B50} = 101 \mu\text{m}$. Export of suspended sand outside the channel margins to the adjacent floodplain occurs during high discharges and associated enhanced water stages (Asselman & Middelkoop, 1998; Nicholas & Walling, 1996; Nittrouer & Viparelli, 2014). According to the Rouse number (Pn) estimates here, fine sand fractions are likely transported to the bank locations as a part of suspension mode for a wide range of shear velocity (u_*) values, even for relatively low u_* values corresponding to moderate water discharge conditions at the delta apex of $Q \sim 1,000 \text{ m}^3 \text{ s}^{-1}$ (Figures 3 and 7). Hence, such moderate discharges are sufficient for conveying bed-material sediment from the main deltaic channels to adjacent wetlands. Similarly, sediment accumulation during low to moderate discharge conditions is observed on subaqueous levees of the supply dominated Wax Lake and Atchafalaya deltas (Mississippi River, USA; Heerden, Wells, & Roberts, 1983; Shaw & Mohrig, 2014). However, transport of suspended sediment to the wetlands and neighbouring water bodies depends on hydraulic connectivity to the main channels (Citterio & Piégay, 2009).

Increased water discharges and elevation levels favour the hydraulic connectivity between the main channels and adjacent wetlands (Heiler, Hein, Schiemer, & Bornette, 1995) and therefore enhance sediment conveyance from the main channel to the deltaic plain (Shen et al., 2015). Due to the decreased frequency of high discharge events ($Q > 1,350 \text{ m}^3 \text{ s}^{-1}$; Figure 3), as well as the decreased magnitude of annual high flow conditions over the past two decades

(Törnqvist et al., 2014), floodplain lakes could remain disconnected from the delta's main channels for longer time intervals. Additionally, a considerable area of the Selenga River delta (i.e., within $\sim 9 \text{ km}$ from the delta outlets; Dong et al., 2016) is impacted by backwater flow, where the range of water stage variability is limited, and the entire channel perimeter is persistently wetted even during low water discharge conditions, thus favouring hydraulic connectivity between the main channels and the surrounding water bodies. Here, connectivity can be facilitated by tie channels and/or exchange of water at the channel–wetland interface, where levees of the main channel are developing and remain below the water line. In such circumstances, the rate of water and sediment exchange with the adjacent wetlands depends on flow velocity at the channel–wetland interface (Hu, Ji, & Guo, 2010; Shiono & Knight, 1991). Moreover, because of the low shear stress conditions within the backwater zone, the delta still maintains the capability of trapping sediment even for conditions of moderate to relatively high discharge ($750\text{--}1,250 \text{ m}^3 \text{ s}^{-1}$, Figure 3).

In general, high flow events can cause rapid remobilization and flushing of the sediment storage within the channel margins (Pietroń et al., 2015). If not eroded due to such rapidly increasing flow conditions, the fresh and cohesive deposit can consolidate during time periods of a few days to 1 or 2 weeks, depending on sediment properties (Parchure & Mehta, 1985). As the water content decreases in the stored sediment during its consolidation, the critical shear velocity to erode this material increases too, which makes it more resistant to changing discharges, wind currents, and lake level changes (Taki, 2000). In the Selenga River delta, consolidation is more common (occurring even under high/bankfull discharges) along higher order channels (e.g., seventh order), where median shear velocities of streamflow are significantly lower ($p \leq .05$; Figure 8) than within the channels of lower order. In addition, the channel network of the Selenga River delta, with its mixture of cohesive sediment (e.g., 72% clay and silt by weight in submerged banks, Section 4.2), likely provides favourable conditions for vegetation to grow and cover accumulated sediment on bars and atop banklines, which offers an additional means to stabilize the sediment deposits. In time, this mechanism fosters net sedimentation so as to sustain and enhance prograding wetlands, thereby facilitating subaerial development of the deposit (Edmonds & Slingerland, 2010).

Recent satellite image analysis on the Selenga River delta channels implies that at $Q = 1,000\text{--}1,500 \text{ m}^3 \text{ s}^{-1}$ (which overlap with the herein considered moderate discharges), water turbidity decreases along the main channels of the delta. Moreover, for $Q > 1,500 \text{ m}^3 \text{ s}^{-1}$, turbidity is decreased (Chalov, Bazilova, et al., 2017). The same image analysis shows that during May and June (beginning of the vegetation growing season in the delta; Lane et al., 2015), turbidity increases, which implies net erosion along the channels. However, in the following months (July and August), bankline vegetation is fully established, and turbidity mostly decreases, which implies net deposition (Figure 9). Hence, it follows that the ability of the delta to store sediment along the channels during various flow conditions may also depend on additional transient factors, such as the evolution of the vegetation cover and seasonal fluctuation of the Lake Baikal water level (see Section 2). In addition, the magnitude of quantified change in water turbidity over the western part of the Selenga River delta (Figure 9, blue curve) is mostly near or in between the corresponding magnitudes over the eastern and

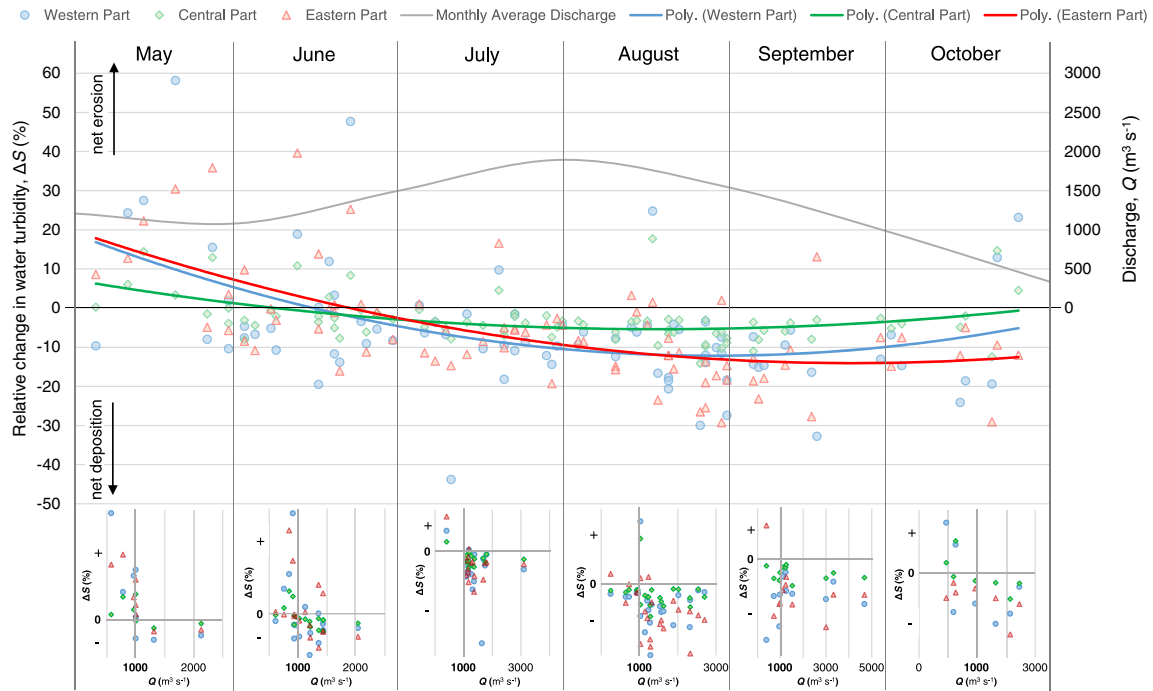


FIGURE 9 Relative change in water turbidity, ΔS (%) along the main channels of the Selenga River delta in western (blue point), central (green diamonds), and eastern (red triangles) parts (see Figure 1b)—data according to Chalov, Bazilova, et al. (2017), ordered by months; bottom inset figures show the same data for specific months ordered by discharge magnitudes at Mostovoy station (Figure 1a). Grey curve indicate monthly average discharges at Mostovoy stations for period 1989–2014

central portions of the delta (red and green curves, respectively). This indicates that the storage functions of the western part of the delta (Figure 1) should reflect the average behaviour of the entire delta.

The greatest proportion of clay and silt (97%) was found within the Selenga River delta floodplain lakes (active and closed), which are located several hundred meters from the main channels. This observation is consistent with other studies that show increasing proportions of clay and silt corresponding to increasing distances from the adjacent channels (Farrell, 1987; Cazanacılı & Smith, 1998). Due to impaired connectivity between closed lakes and channels, the input of fine sediment to lakes is facilitated during flood events (Hill, Lewis, Desmarais, Kauppaymuthoo, & Rais, 2001; Lane et al., 2015). This is particularly the case if a tie channel connects the lake to the distributary channel (Rowland et al., 2009), or if the channel discharge shifts due to, for example, an avulsion or crevasse splay. Generally, flooding dynamics govern the net accumulation rates of delta plains, such as the Mekong River delta, which stores on average 28% of the incoming sediment load (Szczeniński et al., 2013). The Selenga River delta can store as much as 34% of the incoming suspended sediment load (and 67% of the total sediment load) during high flow conditions ($Q \sim 3,000 \text{ m}^3 \text{ s}^{-1}$; Chalov, Thorslund, et al., 2017), likely due to an increase in connectivity between channels and floodplain water bodies. Interestingly, sand fractions are measured in all of the herein measured floodplain lakes, which indicate that it may be conveyed during overbank floods (Kleinhans, Ferguson, Lane, & Hardy, 2013). The sand found in floodplain lakes likely originated by conveyance of suspended load from the channel flow that, as measured in this study, contains on average 7.3% sand.

The clay content of sediment deposited in the Selenga River delta was positively correlated with the measured OM (Figure 4), which suggests that part of the fine sediment could have been deposited in the

form of flocs bonded by organic matter (Droppo, Leppard, Flannigan, & Liss, 1997). The poor sorting of the sediment (Section 4.2) also implicates floc development during transport (Mendenhall, 1930). The flocculation processes increase settling rates of fine suspended particles and thus favour efficient trapping of this material and associated pollutants in the delta (see Kranck, 1981).

Previous studies showed that the suspended sediment load in the Selenga River system (including the delta) is commonly associated with relatively high amounts of metal contaminants, for instance, because high pH conditions of the water limits metal dissolution (Lychagin et al., 2017; Thorslund et al., 2012, 2016). Furthermore, observations show that, once the Selenga River enters its delta area, total metal concentration tends to decrease along small wetland-dominated channels, reducing metal concentration by 77–99% during both moderate and high flow conditions, as considered herein ($Q \sim 1,000$ and $Q \sim 3,000 \text{ m}^3 \text{ s}^{-1}$, respectively; Chalov, Thorslund, et al., 2017). The results of this study show that the submerged bank locations also accumulate various fractions of sediment sizes, even during moderate water discharge conditions. Hence, the submerged bank and connected marshland locations in the backwater zone may also act as active sinks for various metals. The sedimentation patterns and processes of the Selenga River delta add evidence to the capacity of wetland-dominated channels to filter metals (Chalov, Thorslund, et al., 2017).

6 | CONCLUSIONS

A Rouse number (Ph) analysis shows that, even under low to intermediate flow conditions (i.e., low shear velocities), bed material and wash load transported within the main channel can be conveyed via

suspension to adjacent water bodies (i.e., wetlands and lakes) within the backwater reach of the Selenga River delta. Due to ongoing hydroclimatic changes in the Selenga River catchment, the frequency of moderate flows ($Q = 750\text{--}1,250\text{ m}^3\text{ s}^{-1}$) has increased in the Selenga River during the past decades, whereas the frequency of high flows ($Q > 1,350\text{ m}^3\text{ s}^{-1}$) has decreased. Nevertheless, Rouse analyses indicate that, despite the changes in ambient water discharge conditions, sediment is still trapped within the banks and water bodies located in the backwater zone of the Selenga River delta. On the other hand, the export of sediment from the channel to floodplain lakes, which depends on increasingly rare high flow events, has likely diminished. The above outcomes are likely important for future studies on deltaic storage processes of sediment and associated contaminants under conditions of hydroclimatic change.

ACKNOWLEDGMENTS

This study was funded through the EU 7th framework programme Marie Curie Actions – International Research Staff Exchange “FLUMEN” (Grant Agreement: PIRSES-GA-2012-318969), the Swedish Research Council Formas (Project 2012-790), and research support grant from the Bert Bolin Centre and Climate Research School. The work of co-authors affiliated with Lomonosov Moscow State University was supported by Russian Scientific Foundation (project 14-27-00083). Additionally field visits of Russian group were supported by Russian Geographical Society-Russian Foundation for Basic Research project ‘Geochemical barriers in freshwater deltas of Russia’. Laboratory analysis were done under Russian Foundation for Basic Research (project 15-05-05515). Support was provided to J. A. N. through the National Science Foundation (U.S.A.), Grant EAR-1415944. The authors would also like to thank all the people from Lomonosov Moscow State University and Institute of Geography SB RAS in Irkutsk (i.e., Elena Ilycheva and Maxim Pavlov) that helped in the logistics and field measurements.

ORCID

Jan Pietroń  <http://orcid.org/0000-0001-5059-0326>

REFERENCES

- Asselman, N. E., & Middelkoop, H. (1998). Temporal variability of contemporary floodplain sedimentation in the Rhine-Meuse Delta, The Netherlands. *Earth Surface Processes and Landforms*, 23, 595–609. [https://doi.org/10.1002/\(SICI\)1096-9837\(199807\)23:7%3C595::AID-ESP869%3E3.0.CO;2-Y](https://doi.org/10.1002/(SICI)1096-9837(199807)23:7%3C595::AID-ESP869%3E3.0.CO;2-Y)
- Bates, C. D., Coxon, P., & Gibbard, P. L. (1978). A new method for the preparation of clay-rich sediment samples for palynological investigation. *New Phytologist*, 81(2), 459–463.
- Bazhenova, O. I., & Kobylkin, D. V. (2013). The dynamics of soil degradation processes within the Selenga basin at the agricultural period. *Geography and Natural Resources*, 34, 221–227. <https://doi.org/10.1134/S1875372813030050>
- Botter, G., Basso, S., Rodriguez-Iturbe, I., & Rinaldo, A. (2013). Resilience of river flow regimes. *Proceedings of the National Academy of Sciences*, 110(32), 12925–12930. <https://doi.org/10.1073/pnas.1311920110>
- Cahoon, D. R., White, D. A., & Lynch, J. C. (2011). Sediment infilling and wetland formation dynamics in an active crevasse splay of the Mississippi River delta. *Geomorphology*, 131(3), 57–68. <https://doi.org/10.1016/j.geomorph.2010.12.002>
- Cazanacli, D., & Smith, N. D. (1998). A study of morphology and texture of natural levees—Cumberland Marshes, Saskatchewan, Canada. *Geomorphology*, 25, 43–55. [https://doi.org/10.1016/S0169-555X\(98\)00032-4](https://doi.org/10.1016/S0169-555X(98)00032-4)
- Chalov, S. R., Bazilova, V. O., & Tarasov, M. K. (2017). Suspended sediment balance in Selenga delta at the late XX–early XXI century: Simulation by LANDSAT satellite images. *Water Resources*, 44(3), 463–470. <https://doi.org/10.1134/S0097807817030071>
- Chalov, S. R., Jarsjö, J., Kasimov, N. S., Romanchenko, A. O., Pietroń, J., Thorslund, J., & Promakhova, E. V. (2015). Spatio-temporal variation of sediment transport in the Selenga River Basin, Mongolia and Russia. *Environmental Earth Sciences*, 73, 663–680. <https://doi.org/10.1007/s12665-014-3106>
- Chalov, S. R., Thorslund, J., Kasimov, N., Aybullatov, D., Ilyicheva, E., Karthe, D., ... Jarsjö, J. (2017). The Selenga River delta: A geochemical barrier protecting Lake Baikal waters. *Regional Environmental Change*, 17(7), 2039–2053. <https://doi.org/10.1007/s10113-016-0996-1>
- Citterio, A., & Piégay, H. (2009). Overbank sedimentation rates in former channel lakes: Characterization and control factors. *Sedimentology*, 56(2), 461–482. <https://doi.org/10.1111/j.1365-3091.2008.00979.x>
- Colby, B. R. (1957). Relationship of unmeasured sediment discharge to mean velocity. *Transactions, American Geophysical Union*, 38(5), 708. <https://doi.org/10.1029/TR038i005p00708>
- Créteux, J. F., Jelinski, W., Calmant, S., Kouraev, A., Vuglinski, V., Bergé-Nguyen, M., ... Maisongrande, P. (2011). SOLS: A lake database to monitor in the Near Real Time water level and storage variations from remote sensing data. *Advances in Space Research*, 47(9), 1497–1507. <https://doi.org/10.1016/j.asr.2011.01.004>
- Day, J. W., Martin, J. F., Cardoch, L., & Templet, P. H. (1997). System functioning as a basis for sustainable management of deltaic ecosystems. *Coastal Management*, 25, 115–153. <https://doi.org/10.1080/08920759709362315>
- Dean, R. G., Wells, J. T., Fernando, H. J., & Goodwin, P. (2013). Sediment diversions on the lower Mississippi River: Insight from simple analytical models. *Journal of Coastal Research*, 30(1), 13–29. <https://doi.org/10.2112/JCOASTRES-D-12-00252.1>
- Delteus, Å., & Kristiansson, J. (Eds.) (1995). *Kompedium i jordartsanalys: Laboratorieanvisningar. Quaternaria ser. B(1)*. (pp. 20–40) Stockholm.
- Dietrich, W. E. (1982). Settling velocity of natural particles. *Water Resources Research*, 18, 1615–1626. <https://doi.org/10.1029/WR018i006p01615>
- Dong, T. Y., Nittrouer, J. A., Il'icheva, E., Pavlov, M., McElroy, B., Czapiga, M. J., Ma, H., & Parker, G. (2016). Controls on gravel termination in seven distributary channels of the Selenga River Delta, Baikal Rift basin, Russia. *Geological Society of America Bulletin*, (in press). <https://doi.org/10.1130/B31427.1>
- Droppo, I. G., Leppard, G. G., Flannigan, D. T., & Liss, S. N. (1997). The freshwater floc: A functional relationship of water and organic and inorganic floc constituents affecting suspended sediment properties. *Water, Air, and Soil Pollution*, 99(1–4), 43–54. <https://doi.org/10.1023/A:1018359726978>
- Edmonds, D. A., & Slingerland, R. L. (2010). Significant effect of sediment cohesion on delta morphology. *Nature Geoscience*, 3(2), 105–109. <https://doi.org/10.1038/ngeo730>
- Farrell, K. M. (1987). Sedimentology and facies architecture of overbank deposits of the Mississippi River, False River region, Louisiana. *Journal of Sedimentary Petrology*, 57, 111–120.
- Fischer, S., Pietroń, J., Bring, A., Thorslund, J., & Jarsjö, J. (2017). Present to future sediment transport of the Brahmaputra River: Reducing uncertainty in predictions and management. *Regional Environmental Change*, 17(2), 515–526. <https://doi.org/10.1007/s10113-016-1039-7>
- Folk, R. L., & Ward, W. C. (1957). Brazos River bar: A study in the significance of grain size parameters. *Journal of Sedimentary Research*, 27(1).
- Gasparotto, E., Malo, D.D., & Gelderman, R.H. (2003). Impact of organic matter removal on particle size analysis by pipette and hydrometer. Soil/Water Research, 2003 Progress Report, South Dakota State University, Brookings, SD

- Gutry-Korycka, M., & Werner-Więckowska, H. (1996). Przewodnik do hydrograficznych badań terenowych. Wydawnictwo Naukowe PWN, Warszawa.
- Hack, J. T. (1957). Studies of longitudinal stream profiles in Virginia and Maryland: U.S. Geological Survey Professional Paper 294-B, 59 p
- Heerden, I. L. V., Wells, J. T., & Roberts, H. H. (1983). River-dominated suspended-sediment deposition in a new Mississippi Delta. *Canadian Journal of Fisheries and Aquatic Sciences*, 40(S1), 60–71.
- Heiler, G., Hein, T., Schiemer, F., & Bornette, G. (1995). Hydrological connectivity and flood pulses as the central aspects for the integrity of a river-floodplain system. *Regulated Rivers: Research & Management*, 11(3–4), 351–361. <https://doi.org/10.1002/rrr.3450110309>
- Hill, P. R., Lewis, C. P., Desmarais, S., Kauppaymuthoo, V., & Rais, H. (2001). The Mackenzie Delta: Sedimentary processes and facies of a high-latitude, fine-grained delta. *Sedimentology*, 48(5), 1047–1078. <https://doi.org/10.1046/j.1365-3091.2001.00408.x>
- Hu, C., Ji, Z., & Guo, Q. (2010). Flow movement and sediment transport in compound channels. *Journal of Hydraulic Research*, 48(1), 23–32. <https://doi.org/10.1080/00221680903568600>
- Huston, D. (2014). Particulate organic carbon trapping efficiency in the stream bed for cobbles and gravels: A laboratory test. *Kaleidoscope*, 11(1), 73.
- Hydroweb (2017). Time series of water levels in the rivers and lakes around the world [Online]: <http://hydroweb.theia-land.fr/>, Accessed: October 2017
- Ilyicheva, E. I., Gagarinova, O. V., & Pavlov, M. V. (2015). Hydrogeomorphological analysis of landscape formation within the Selenga River delta. *Geography and Natural Resources*, 36, 263–270. <https://doi.org/10.1134/S1875372815030063>
- Jalowska, A. M., Rodríguez, A. B., & McKee, B. A. (2015). Responses of the Roanoke Bayhead Delta to variations in sea level rise and sediment supply during the Holocene and Anthropocene. *Anthropocene*, 9, 41–55. <https://doi.org/10.1016/j.ancene.2015.05.002>
- Jarsjö, J., Chalov, S. R., Pietroń, J., Alekseenko, A., & Thorslund, J. (2017). Patterns of soil contamination, erosion, and river loading of metals in a gold mining region of Northern Mongolia. *Regional Environmental Change*, 17(7), 1991–2005. <https://doi.org/10.1007/s10113-017-1169-6>
- Kleinhans, M. G., Ferguson, R. I., Lane, S. N., & Hardy, R. J. (2013). Splitting rivers at their seams: Bifurcations and avulsion. *Earth Surface Processes and Landforms*, 38(1), 47–61. <https://doi.org/10.1002/esp.3268>
- Kranck, K. (1981). Particulate matter grain-size characteristics and flocculation in a partially mixed estuary. *Sedimentology*, 28(1), 107–114. <https://doi.org/10.1111/j.1365-3091.1981.tb01667.x>
- Krumbein, W. C., & Aberdeen, E. (1937). The sediments of Barataria bay. *Journal of Sedimentary Research*, 7(1).
- Lane, C. R., Anenkhonov, O., Liu, H., Autrey, B. C., & Chepinoga, V. (2015). Classification and inventory of freshwater wetlands and aquatic habitats in the Selenga River Delta of Lake Baikal, Russia, using high-resolution satellite imagery. *Wetlands Ecology and Management*, 23, 195–214. <https://doi.org/10.1007/s11273-014-9369-z>
- Leeder, M. R., Harris, T., & Kirkby, M. J. (1998). Sediment supply and climate change: Implications for basin stratigraphy. *Basin Research*, 10, 7–18. <https://doi.org/10.1046/j.1365-2117.1998.00054.x>
- Loeche, M. (2014). RgoogleMaps: Overlays on Google Map Tiles in R. R package version 1.2.0.6, URL <http://CRAN.R-project.org/package=RgoogleMaps>.
- Lychagin, M., Chalov, S., Kasimov, N., Shinkareva, G., Jarsjö, J., & Thorslund, J. (2017). Surface water pathways and fluxes of metals under changing environmental conditions and human interventions in the Selenga River system. *Environmental Earth Sciences*, 76(1), 1. <https://doi.org/10.1007/s12665-016-6304-z>
- Lynds, R. M., Mohrig, D., Hajek, E. A., & Heller, P. L. (2014). Paleoslope reconstruction in sandy suspended-load-dominant rivers. *Journal of Sedimentary Research*, 84(10), 825–836. <https://doi.org/10.2110/jsr.2014.60>
- Mendenhall W.C. (1930). Lithologic studies of sedimentary rocks of Black Hills Region. In: Shorter contributions to general geology, 1930. U.S. Geol. Surv., Profess. Papers 165(e), 31–32
- Meyers, P. A., & Ishiwatari, R. (1993). Lacustrine organic geochemistry—An overview of indicators of organic matter sources and diagenesis in lake sediments. *Organic Geochemistry*, 20(7), 867–900. [https://doi.org/10.1016/0146-6380\(93\)90100-P](https://doi.org/10.1016/0146-6380(93)90100-P)
- Middleton, G. V., & Southard, J. B. (1984). Mechanics of Sediment Movement. SEPM Short Course Notes (2nd ed., Vol. 3). SEPM (Society for Sedimentary Geology).
- Mjos, R., Walderhaug, O., & Prestholm, E. (1993). Crevasse-splay sandstone geometries in the Middle Jurassic Ravenscar Group of Yorkshire, UK. In M. Marzo, & C. Puigdefabregas (Eds.), *Alluvial sedimentation* (Vol. 17) *Int. Assoc. Sedimentol. Spec. Publ* (pp. 167–184).
- Nicholas, A. P., & Walling, D. E. (1996). The significance of particle aggregation in the overbank deposition of suspended sediment on river floodplains. *Journal of Hydrology*, 186(1–4), 275–293. [https://doi.org/10.1016/S0022-1694\(96\)03023-5](https://doi.org/10.1016/S0022-1694(96)03023-5)
- Nilsson, C., Reidy, C. A., Dynesius, M., & Revenga, C. (2005). Fragmentation and flow regulation of the world's large river systems. *Science*, 308(5720), 405–408. <https://doi.org/10.1126/science.1107887>
- Nittrouer, J. A., Best, J. L., Brantley, C., Cash, R. W., Czapiga, M., Kumar, P., & Parker, G. (2012). Mitigating land loss in coastal Louisiana by controlled diversion of Mississippi River sand. *Nature Geoscience*, 5, 534–537. <https://doi.org/10.1038/ngeo1525>
- Nittrouer, J. A., Mohrig, D., & Allison, M. A. (2011). Punctuated sand transport in the lowermost Mississippi River. *Journal of Geophysical Research*, 116, 1914–1934. <https://doi.org/10.1029/2011JF002026>
- Nittrouer, J. A., & Viparelli, E. (2014). Sand as a stable and sustainable resource for nourishing the Mississippi River delta. *Nature Geoscience*, 7(5), 350–354. <https://doi.org/10.1038/ngeo2142>
- Parchure, T. M., & Mehta, A. J. (1985). Erosion of soft cohesive sediment deposits. *Journal of Hydraulic Engineering*, 111(10), 1308–1326. [https://doi.org/10.1061/\(ASCE\)0733-9429\(1985\)111:10\(1308\)](https://doi.org/10.1061/(ASCE)0733-9429(1985)111:10(1308))
- Parker, G. (1991). Selective sorting and abrasion of river gravel. I: Theory. *Journal of Hydraulic Engineering*, 117(2), 131–147. [https://doi.org/10.1061/\(ASCE\)0733-9429\(1991\)117:2\(131\)](https://doi.org/10.1061/(ASCE)0733-9429(1991)117:2(131))
- Pietroń, J., Chalov, S. R., Chalova, S. A., Alekseenko, A. V., & Jarsjö, J. (2017). Extreme spatial variability in soil degradation and riverine sediment load inputs from surface mining areas in the headwaters of the Lake Baikal Basin. *Catena*, 152, 82–93. <https://doi.org/10.1016/j.catena.2017.01.008>
- Pietroń, J., Jarsjö, J., Romanchenko, A. O., & Chalov, S. R. (2015). Model analyses of the contribution of in-channel processes to sediment concentration hysteresis loops. *Journal of Hydrology*, 527, 576–589. <https://doi.org/10.1016/j.jhydrol.2015.05.009>
- Potemkina, T. G. (2011). Sediment runoff formation trends of major tributaries of Lake Baikal in the 20th century and at the beginning of the 21st century. *Russian Meteorology and Hydrology*, 36(12), 819–825. <https://doi.org/10.3103/S1068373911120077>
- Rowland, J. C., Dietrich, W. E., Day, G., & Parker, G. (2009). Formation and maintenance of single-thread tie channels entering floodplain lakes: Observations from three diverse river systems. *Journal of Geophysical Research*, 114, F02013. <https://doi.org/10.1029/2008JF001073>
- Seward-Thompson, B. L., & Hails, J. R. (1973). An appraisal of the computation of statistical parameters in grain size analysis. *Sedimentology*, 20(1), 161–169. <https://doi.org/10.1111/j.1365-3091.1973.tb01612.x>
- Shaw, J. B., & Mohrig, D. (2014). The importance of erosion in distributary channel network growth, Wax Lake Delta, Louisiana, USA. *Geology*, 42(1), 31–34. <https://doi.org/10.1130/G34751.1>
- Shein, E. V. (2009). The particle-size distribution in soils: Problems of the methods of study, interpretation of the results, and classification.

- Eurasian Soil Science*, 42(3), 284–291. <https://doi.org/10.1134/S1064229309030053>
- Shen, Z., Törnqvist, T. E., Mauz, B., Chamberlain, E. L., Nijhuis, A. G., & Sandoval, L. (2015). Episodic overbank deposition as a dominant mechanism of floodplain and delta-plain aggradation. *Geology*, 43(10), 875–878. <https://doi.org/10.1130/G36847.1>
- Shiono, K., & Knight, D. W. (1991). Turbulent open-channel flows with variable depth across the channel. *Journal of Fluid Mechanics*, 222, 617–646. <https://doi.org/10.1017/S0022112091001246>
- Simon Fraser University. (2012). Experimental procedures: Hydrometer method with photos. Soil Science Lab, Simon Fraser University, Burnaby, BC.
- Stern, M., Flint, L., Minear, J., Flint, A., & Wright, S. (2016). Characterizing changes in streamflow and sediment supply in the Sacramento River Basin, California, using hydrological simulation program—FORTRAN (HSPF). *Water*, 8(10), 432. <https://doi.org/10.3390/w8100432>
- Syvitski, J. P. M., Kettner, A. J., Overeem, I., Hutton, E. W., Hannon, M. T., Brakenridge, G. R., ... Nicholls, R. J. (2009). Sinking deltas due to human activities. *Nature Geoscience*, 2(10), 681. <https://doi.org/10.1038/ngeo629>
- Syvitski, J. P. M., Overeem, I., Brakenridge, G. R., & Hannon, M. (2012). Floods, floodplains, delta plains — A satellite imaging approach. *Sedimentary Geology*, 267, 1–14. <https://doi.org/10.1016/j.sedgeo.2012.05.014>
- Syvitski, J. P. M., & Saito, Y. (2007). Morphodynamics of deltas under the influence of humans. *Global and Planetary Change*, 57, 261–282. <https://doi.org/10.1016/j.gloplacha.2006.12.001>
- Syvitski, J. P. M., Vörösmarty, C. J., Kettner, A. J., & Green, P. (2005). Impact of humans on the flux of terrestrial sediment to the global coastal ocean. *Science*, 308(5720), 376–380. <https://doi.org/10.1126/science.1109454>
- Szczuciński, W., Jagodziński, R., Hanebuth, T. J., Statterger, K., Wetzel, A., Mitrega, M., ... Van Phach, P. (2013). Modern sedimentation and sediment dispersal pattern on the continental shelf off the Mekong River delta, South China Sea. *Global and Planetary Change*, 110, 195–213. <https://doi.org/10.1016/j.gloplacha.2013.08.019>
- Taki, K. (2000). Critical shear stress for cohesive sediment transport. *Proceedings in Marine Science*, 3, 53–61. [https://doi.org/10.1016/S1568-2692\(00\)80112-6](https://doi.org/10.1016/S1568-2692(00)80112-6)
- Thorslund, J., Jarsjö, J., Chalov, S. R., & Belozerova, E. V. (2012). Gold mining impact on riverine heavy metal transport in a sparsely monitored region: The upper Lake Baikal Basin case. *Journal of Environmental Monitoring*, 14(10), 2780–2792. <https://doi.org/10.1039/c2em30643c>
- Thorslund, J., Jarsjö, J., Jaramillo, F., Jawitz, J. W., Manzoni, S., Basu, N. B., ... Destouni, G. (2017). Wetlands as large-scale nature-based solutions: Status and challenges for research, engineering and management. *Ecological Engineering*, 108(B), 489–497. <https://doi.org/10.1016/j.ecoleng.2017.07.012>
- Thorslund, J., Jarsjö, J., Wällstedt, T., Mörtz, C. M., Lychagin, M. Y., & Chalov, S. R. (2016). Speciation and hydrological transport of metals in non-acidic river systems of the Lake Baikal basin: Field data and model predictions. *Regional Environmental Change*. <https://doi.org/10.1007/s10113-016-0982-7>
- Törnqvist, R., Jarsjö, J., Pietróń, J., Bring, A., Rogberg, P., Asokan, S. M., & Destouni, G. (2014). Evolution of the hydro-climate system in the Lake Baikal basin. *Journal of Hydrology*, 519, 1953–1962. <https://doi.org/10.1016/j.jhydrol.2014.09.074>
- Townend, J. (2013). Practical statistics for environmental and biological scientists. John Wiley & Sons, 189–190
- U.S. Geological Survey. (2012). U.S. Geological Survey. Earth Explorer. [Online]: <http://earthexplorer.usgs.gov/>, Accessed: January 2012.
- U.S. Geological Survey. (2015). U.S. Geological Survey. Earth Explorer. [Online]: <http://earthexplorer.usgs.gov/>, Accessed: November 2015.
- Wentworth, C. K. (1922). A scale of grade and class terms for clastic sediments. *The Journal of Geology*, 30(5), 377–392.
- Wright, L. D., & Coleman, J. M. (1972). River delta morphology: Wave climate and the role of the subaqueous profile. *Science*, 176, 282–284. <https://doi.org/10.1126/science.176.4032.282>
- Yang, S. L., Milliman, J. D., Li, P., & Xu, K. (2011). 50,000 dams later: Erosion of the Yangtze River and its delta. *Global and Planetary Change*, 75, 14–20. <https://doi.org/10.1016/j.gloplacha.2010.09.006>
- Yang, S. L., Zhang, J., Zhu, J., Smith, J. P., Dai, S. B., Gao, A., & Li, P. (2005). Impact of dams on Yangtze River sediment supply to the sea and delta intertidal wetland response. *Journal of Geophysical Research*, 110, F03006. <https://doi.org/10.1029/2004JF000271>
- Zhao, Y., Zou, X., Gao, J., Xu, X., Wang, C., Tang, D., ... Wu, X. (2015). Quantifying the anthropogenic and climatic contributions to changes in water discharge and sediment load into the sea: a case study of the Yangtze River, China. *Science of the Total Environment*, 536, 803–812. <https://doi.org/10.1016/j.scitotenv.2015.07.119>

SUPPORTING INFORMATION

Additional Supporting Information may be found online in the supporting information tab for this article.

How to cite this article: Pietróń J, Nitttrouer JA, Chalov SR, et al. Sedimentation patterns in the Selenga River delta under changing hydroclimatic conditions. *Hydrological Processes*. 2018;1–15. <https://doi.org/10.1002/hyp.11414>